Electrochimica Acta 104 (2013) 302–307

Electrochimica Acta

journal homepage: www.elsevier.com/locate/electacta

Synthesis of a novel ferrocene-contained polypyrrole derivative and its performance as a cathode material for Li-ion batteries

Chang Su, Lingmin Wang, Lihuan Xu, Cheng Zhang*

State Key Laboratory Breeding Base of Green Chemistry-Synthesis Technology, International Sci. &Tech. Cooperation Base of Energy Materials and Application, College of Chemical Engineering and Materials Science, Zhejiang University of Technology, Hangzhou, 310014, PR China

ARTICLE INFO

Article history:
Received 27 December 2012
Received in revised form 15 April 2013
Accepted 20 April 2013
Available online 4 May 2013

Keywords:
Lithium ion battery
Ferrocene derivative
Polypyrrole
Electrochemical characteristic

ABSTRACT

A novel ferrocene-contained pyrrole, 4-(1H-pyrrol-1-yl) phenyl ferrocenecarboxylate (FcPy) was synthesized by esterification of 4-(1H-pyrrol-1-yl) phenol (PLPY) and ferrocenecarboxylic acid. Then the homopolymer of FcPy (PFcPy), copolymer of FcPy and pyrrole (P(FcPy-co-Py)), polypyrrole (PPy) were prepared by chemical oxidative polymerization. And the structure, morphology, electrochemical properties of prepared polymers were characterized by fourier transform infrared spectroscopy (FTIR), scanning electron microscopy (SEM), cyclic voltammograms (CV) and electrochemical impedance spectra (EIS), respectively. Also, the charge/discharge properties of the prepared polymers were studied by galvanostatic charge–discharge testing. The results demonstrated that the introduction of ferrocene to polypyrrole obviously improved the specific capacity of PPy cathode and gave a well-defined plateau at the potential rang of about 3.5 V. Under our experimental conditions, the discharge capacity of undoped PPy-based electrodes only presented 16.5 mAh g^{-1} at 20 mA g^{-1} between 2.5 and 4.2 V, while PFcPy-based electrodes exhibited an initial discharge capacity of up to 43.2 mAh g^{-1}. Specially, the P(FcPy-co-Py)-based electrodes even showed a discharge capacity of 68.1 mAh g^{-1} and the improved discharge platform, which were ascribed to the resonance doping effect of pendant group, the advanced electrochemical nature of ferrocene moiety and the loose morphology of copolymer.

1. Introduction

In recent years, one of the most challenges in modern society is to find a suitable power that will satisfy our growing portable power requirements with the developing of electronic products. Li-ion batteries, as demonstrated by their wide applications in portable electronic devices, have been considered to be the most promising technology in the future [1–3]. Whereas, the wide use of this technology is mainly restricted by the positive electrode, which usually shows a much lower capacity than that of the negative one. Therefore, many attempts have been paid to the development of a promising positive electrode with high capacity and high stability. Currently, many effects mainly focus on the inorganic transition-metal-oxide-based materials (such as $LiCoO_2$, $LiMn_2O_4$, $LiFePO_4$ and V_2O_5, etc.), which have a series of disadvantages, such as limited mineral resources and waste treatment process. In addition, the high energy demand and CO_2 emissions during the producing process also limit their large scale applications for upcoming electric vehicles and renewable power stations [4–6]. Therefore, the novel cathode materials are still highly desired for the development of advanced Li-ion batteries. To address this issue, one of the most attractive approaches is the utilization of organic cathode materials [7–9] because of their easy preparation and high energy density, as well as a possibility for the design of any size and shape of electrode films for flexible Li-ion batteries, although they have some known problems, such as relatively poor performances in capacity and stability, and others. So far, several types of organic positive-electrode materials have been proposed, mainly including of electroactive conducting polymers [7,10], organosulfur polymers [11], nitroxide radical tetramethylpiperidine-N-oxyl (TEMPO)-based polymers [12,13], pendant-type polymer based on ferrocene and carbazole [14,15], aromatic carbonyl derivatives and quinine-based materials [16], etc.

Among them, conducting polymers seem to be a most probable candidate because of their high electronic conductivity and reversible redox-active chemistry. In particular, p-doped polymers such as polyaniline (PAn) [17], polypyrrole (PPy) [18,19], polythiophene (PTh) [20,21], and their derivatives are frequently reported as organic cathode materials for rechargeable batteries. These polymers can be charged and discharged by a redox reaction, which

* Corresponding author.
E-mail address: czhang@zjut.edu.cn (C. Zhang).

0013-4686
http://dx.doi.org/10.1016/j.electacta.2013.04.127

companies an inserted/de-inserted process of both lithium ions and counter anions in the electrolyte. Among the conducting polymers, PPy is one of the most popular for use as a cathode, because of its environmental stability, high specific energy (ranging from 80 to 390 Wh kg^{-1}) [7] and theoretical capacity (~400 mAh g^{-1}). However, the electrodes so far synthesized have several problems relating to the generally low realizable capacity (due to the low doping degree) and the sloping charge–discharge curves (due to the nature of doping process), which have limited the practical applications of PPy in energy storage devices.

Ferrocene as an organometallic compound has been extensively investigated as a standard electrode in the redox potential measurement because of its air stability, excellent electrochemical response, redox property, and so on. [22–25] Recently,[14] it has been reported that polymers carrying ferrocene moieties such as poly(vinlferrocene), poly(ethynylferrocene) and poly(ferrocene) have been applied as cathode-active materials in organic lithium ion batteries, which exhibits promising battery properties such as high power density and the stable voltage plateaus (~3.4 V). Moreover, Park's group recently anchored ferrocene groups to the PPy backbone, and the prepared PPy-based copolymer attaching the redox couples demonstrated a flat charge–discharge curve over all capacity range and an additional capacity comparing to that of PPy. [10] The obtained ferrocene modified PPy copolymer is mainly utilized as the coatings to study its effects on improving $LiFePO_4$ performances. However, the detail investigation on the influence of ferrocene on the electrochemical properties of PPy has not been further explored just now.

In this work, a novel ferrocene-containing pyrrole was synthesized, and the homopolymer of FcPy (PFcPy), copolymer of FcPy and pyrrole P(FcPy-co-Py), polypryyole (PPy) were prepared by chemical oxidation polymerization. And the electrochemical properties of above three polymers as cathode materials of lithium ion battery were systematically investigated by lithium ion half-cell method, comparatively. Also, the effects of ferrocene moiety on the performances of the PPy-based cell were investigated. Moreover, the possible mechanism for the improvement of the electrochemical properties was further discussed. In order to eliminate the effects of the uncertainly doping level on the research, the polymers in the study were adopted in the undoped state. Thanks to the introduction of ferrocene-based pendants in PPy backbone, we found that the (PFcPy)- and/or P(FcPy-co-Py)-based electrode remarkably improved discharge voltage plateaus and charge–discharge performance compared to the pristine PPy electrode and were promising as advanced cathode material.

2. Experimental

2.1. Materials

2,5-Dimethoxytetrahydrofuran (98%), 4-aminophenol (98%), pyrrole (99%) were purchased from Aladdin-Reagent Co. Pyrrole was purified by distillation before use. Ferrocene carboxylic acid (99%) was purchased from Energy Chemical Reagent Co. All other reagents were received as analytical grade and used without further purification.

2.2. Synthesis of FcPy

The synthesis of the monomer (FcPy) is shown in Scheme 1.

2.2.1. Synthesis of 4-(1H-pyrrol-1-yl) phenol

2,5-Dimethoxytetrahydrofuran (6.46 ml, 0.05 mol) and 4-aminophenol (5.4 g, 0.05 mol) were dissolved in a mixture of 20 ml deionized water and 40 ml glacial acetic acid, and heated reflux

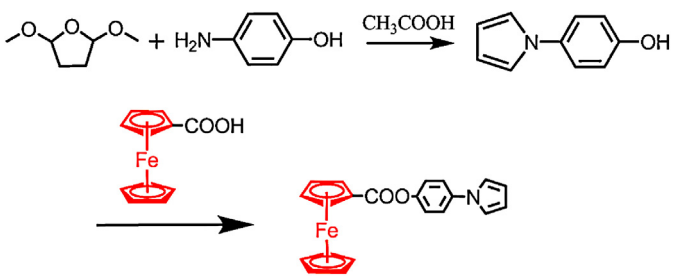

Scheme 1. The synthesis route to FcPy.

(70 °C) for 1 h until the solution turned to jacinth. The reaction mixture was then cooled and extracted with CH_2Cl_2, and the organic fraction was washed with saturated brine for three times. The organic phase was separated, dried, and evaporated to dryness. Flash chromatography of the residue (silica gel, petrol ether/ethyl acetate 20:1) afforded the title compound (3.47 g, 52% yield) as a white powder. ^{1}H NMR ($CDCl_3$, 400 MHz) d/ppm: 4.80 (s, 1H); 7.01 (t, 2H); 6.35 (t, 2H); 6.90 (d, 2H); 7.28 (d, 2H).

2.2.2. Synthesis of FcPy

Ferrocene carboxylic acid (1.518 g) and 4-(1H-pyrrol-1-yl)phenol (0.955 g) were dissolved in the mixture of 40 ml dichlormethane and 25 ml DMF in the pre-dried three-necked flask, then 0.15 g 4-dimethylaminopyridine was added as acylating catalyst and 1.35 g N,N′-dicyclohexylcarbodiimide as dehydrating agent, and stirring for 24 h at room temperature. The reaction mixture was then separated by vacuum filtration. The filtrate was washed with saturated brine for three times. Organic phase was dried over sodium sulfate. The ester was purified by column chromatography using silica gel and petroleum ether/ethyl acetate afforded the title compound as golden flakes like crystals. ^{1}H NMR ($CDCl_3$, 400 MHz) d/ppm: 4.99 (t, 2H), 4.54 (t, 2H), 4.33 (s, 5H), 6.38 (d, 2H), 7.09 (d, 2H), 7.26 (d, 2H), 7.45 (d, 2H).

2.3. Chemical polymerization of PPy, PFcPy and P(FcPy-co-Py)

All of PPy, P(FcPy-co-Py) and PFcPy were prepared by the same methods. Py, FcPy or Py/FcPy monomers (molar ratio of FcPy/Py = 1:5) was dissolved in methanol. $FeCl_3$ $6H_2O$ in methanol ($FeCl_3$ $6H_2O$/[FcPy + Py] molar ratio = 2.5:1) were then slowly added with dropwise. The reaction was conducted under nitrogen atmosphere at room temperature for 24 h. Afterwards, the precipitates were filtered and washed with methanol and deionized water alternately till the filtrate was clear. The polymers were dried under vacuum for 24 h at 60 °C.

2.4. Characterization and electrochemical measurements

FT-IR spectra were carried out on a Nicolet 6700 spectrometer (Thermo Fisher Nicolet, USA) with KBr pellets. UV–vis spectra were recorded on a Varian Cary 100 UV–vis spectrophotometer (Varian, USA). ^{1}H NMR spectra of the compounds were recorded on a Bruker AVANCE III 500 MHz spectrometer (Bruker, Switzer-land) using $CDCl_3$ Scanning electron microscopy (SEM) measurements were taken using a Hitachi S-4800 scanning electron microscope (Hitachi, Japan).

For cathode characterization, CR2032 coin-type cell was used and assembled in an argon-filled glove box. The cathode electrodes were prepared by coating a mixture containing 50% as prepared polymers, 40% acetylene black, 10% PVDF binder on circular Al current collector foils, followed by dried at 60 °C for 10 h. After that, the cells were assembled with lithium foil as the anode, the prepared electrodes as cathode and 1 M $LiPF_6$ dissolved in ethylene carbonate

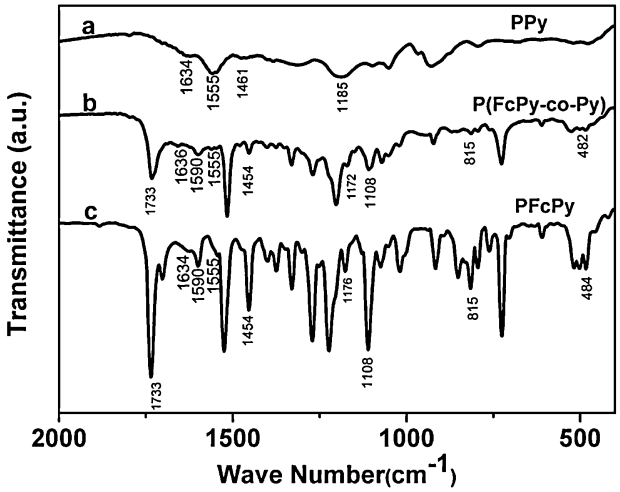

Fig. 1. FTIR spectrum of the (a) PPy, (b) P(FcPy-co-Py) and (c) PFcPy samples.

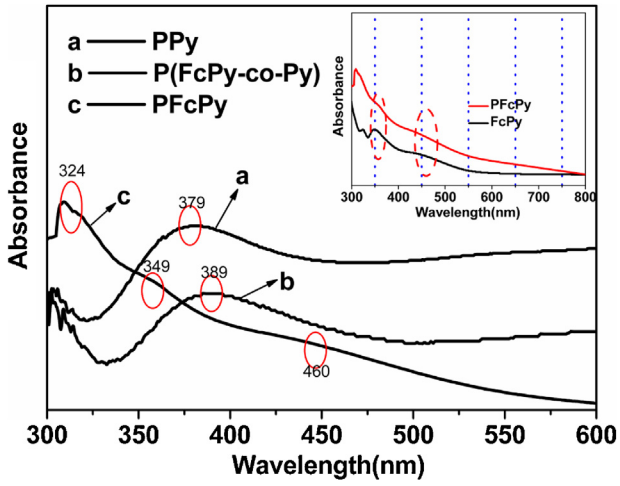

Fig. 2. UV–vis spectra of (a) PPy, (b) P(FcPy-co-Py) and (c) PFcPy. [Inset: UV–vis spectra of PFcPy and FcPy monomer].

(EC) and dimethyl carbonate (DMC) (EC/DMC = 1:1, v/v) as the electrolyte. The charge–discharge measurements were carried out on a LAND CT2001 A in the voltage range of 2.5–4.2 V versus Li/Li^+, using a constant current density at room temperature. Electrochemical Impedance Spectroscopy (EIS) experiments were carried out at open circuit voltage (OCV) of frequency ranges from 0.1 Hz to 1 MHz in CHI 660C electrochemical working station by the assembled stimulant lithium ion half-cells. The cyclic voltammograms (CV) tests were performed with a CHI 660C electrochemical working station in 0.1 M $LiClO_4/CH_3CN$ versus Ag/AgCl at a scan rate of 25 mV s^{-1}.

3. Results and discussion

3.1. Material characterization

Fig. 1 shows the FT-IR spectra of the as-prepared polymers. As can be seen in Fig. 1(a), the absorption peaks of about 1555 cm^{-1} is attributed to the stretching vibration of pyrrole units, and the absorption peaks at 1176–1185 cm^{-1} is due to the C-N stretching of pyrrole units. In Fig. 1(b) and (c), the similar characteristic bands of PPy are presented in P(FcPy-co-Py) and PFcPy. In addition, some new bands can be observed clearly in the spectrum of P(FcPy-co-Py) and PFcPy, in which the absorption peak of 1590 cm^{-1} is ascribed to C=C stretching vibration of benzene ring, while the absorption peak of 1733 cm^{-1} is the stretching of C=O (ester carbonyl). And the absorption peaks at 1108, 815 and 482–484 cm^{-1} are due to mono-substituted ferrocene [26,27]. All those indicate that both pyrrole moieties and ferrocene are included in polymers and the P(FcPy-co-Py) and PFcPy polymers have been successfully prepared.

The UV–vis spectra (normalized absorbance) is further measured in DMF (10^{-3} g/L) to explore on characteristics of PFcPy, P(FcPy-co-Py) and PPy. The curve (a) shows the UV–vis spectra of PPy, in which the absorption peaks at ~379 nm are corresponding to the π-π* electron transition from the pyrrole units of PPy backbone. In Fig. 2(b), we can also find one broad absorption peaks at ~389 nm for P(FcPy-co-Py), which is still attributed to the π-π* electron transition from the pyrrole units. However, the π-π* absorption peak of P(FcPy-co-Py) has a obviously red shift compared to the corresponding peaks of PPy indicating that the electron delocalization in the PPy backbone is enhanced, which can be due to the electron-donating effect of the side benzene group supplied by FcPy unites of P(FcPy-co-Py). This effect, in somg sense, can be considered as a doping process for PPy molecular chain, and as a result, the charge carrier transportation alone the polymer main chain of P(FcPy-co-Py) is improved, which is crucial for high-performance lithium battery. For PFcPy (as shown in Fig. 2(c)), the absorption peaks at ~324 nm and ~460 nm correspond to the π-π* electron transition of the ferrocene moieties, while the absorption peak at ~349 nm is cased by both the phenylene characteristic in the pendant groups and the blue shift π-π* electron transition from the pyrrole units(because of the no mutual conjugation). The inset in the figure compares the UV–vis spcetra of both FcPy monomer and PFcPy polymer. Compared to FcPy monomer, it can be found that the position of the main absorption peak of PFcPy polymer has never changed, and that no new π-π* electron transition peak of PPy molecular chain has been observed. It is possibly caused by the steric bulkiness of the FcPy pendant make it difficult for two neighboring FcPy pendants in PFcPy to array in coplanar fashion. Thereby, no mutual conjugation between two neighboring FcPy pendants is possible for homopolymer PFcPy and the electron delocalization along the polymer backbone becomes ineffective, resulting in the PFcPy polymer shows a similar UV–vis spectra characteristic to that of FcPy monomer. While, for copolymer P(FcPy-co-Py), two neighboring FcPy pendants are separated by Py unit and the conjugation effect has been enhanced. Moreover, the electron delocalization along the copolymer backbone becomes move effective.

The morphologies of the as-obtained polymers have also been investigated by SEM, and the morphology changes for PPy, P(FcPy-co-Py) and PFcPy are shown in Fig. 3. As can be seen in Fig. 3(a), PPy has a dense packing plate-like structure and the aggregation of PPy particles can be noticed obviously. Comparatively, as the ferrocene-based moiety is introduced into PPy, the morphologies of P(FcPy-co-Py) and PFcPy change obviously from that of PPy. Specially, the polymer of P(FcPy-co-Py) shows a loose stacking structure assembled by many smaller particles, as shown in Fig. 3(b). We also measured the specific surface areas of three polymers by BET testing method, and the results of PPy, P(FcPy-co-Py) and PFcPy were found to be 9.4930, 19.3431 and 15.8763 $m^2 g^{-1}$. And this open structure of P(FcPy-co-Py) with the porous morphologies is in favor of the contact of electrode-active material and electrolyte; as a result, much more electrode-active material is effectively utilized and the electrochemical properties of P(FcPy-co-Py) is obviously improved. All of those are very important to prepare a good cathode material for Li-ion batteries. However, as the polymer main chain is thoroughly composted of ferrocene-contained pyrrole units (PFcPy), the loose stacking structure of P(FcPy-co-Py) become aggregate again (as shown in Fig. 3(c)),

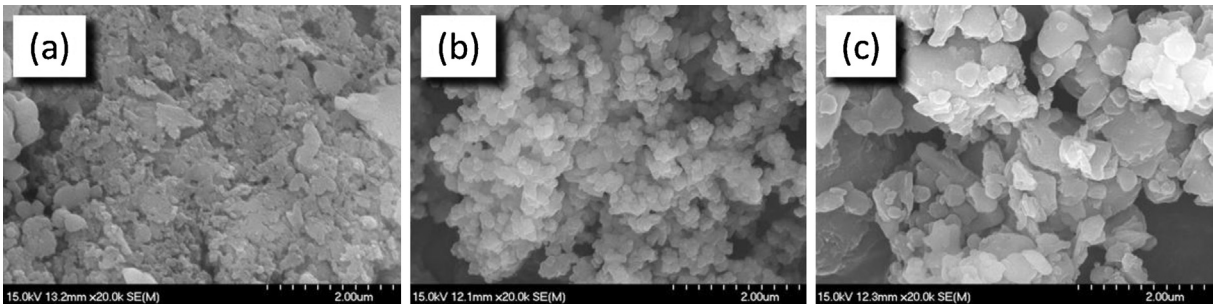

Fig. 3. SEM images of powder samples (a)PPy, (b) P(FcPy-co-Py) and (c) PFcPy.

which can be attributed to the oligomer structure of PFcPy and its poor self-assembly properties.

3.2. Electrochemical performance

Fig. 4 shows the cyclic voltammetry (CV) profile of the PPy, P(FcPy-co-Py) and PFcPy measured in 0.1 M lithium perchlorate/acetonitrile solution. As shown in the figure, the electrode of PPy shows a couple of wide anodic and cathodic peaks at about 0.45 V and 0.34 V, respectively, corresponding to the charge/discharge process of the redox couple of pyrrole. And the approximately symmetrical peaks with the relatively narrow peak-to-peak separation of the anodic and cathodic potential (about 0.11 V) at a scan rate of 25 mV s^{-1} imply the good oxidation/reduction reversibility of the produced PPy active material as cathode. Comparatively, the CV feature of the P(FcPy-co-Py) shows two pairs of reversible redox peaks. One pair of reduction and oxidation peaks appearing at 0.45 and 0.34 V can be assigned to radical cation reaction of pyrrole units during charge/discharge reactions. The other couple of redox peaks appears at 0.82 and 0.65 V, which can be attributed to the redox couple of the organometallic ferrocene units. All those further indicate that both of pyrrole units and ferrocene-contained pyrrole units are all included successfully in the as-prepared copolymer, and two redox couples will be exhibited during the charge/discharge process. However, for the PFcPy, the curve CV feature is quite different, in which the redox peaks of the organometallic ferrocene units are much more significant compared with that of P(FcPy-co-Py), while the redox peaks of the PPy disappear, indicating that the large steric effect of side-chain pendants damages the conjugated structure of pyrrole and seriously impedes redox process of PPy during the chagre-discharge process.

3.3. Charge–discharge performance

The charge–discharge behaviors of the as-prepared polymers as cathode of lithium batteries have been systematically investigated by simulated lithium ion half-cell method. In order to eliminate the effects of some uncertainly doped factors on the researches, the undoped polymers are adopted during the experiment. The initial charge–discharge profiles of the polymers at 20 mA g^{-1} between 2.5 and 4.2 V are shown in Fig. 5. As we can see from Fig. 5(a), the undoped PPy shows an initial discharge capacity of 16.5 mAh g^{-1} at initial cycle by stimulated lithium ion half-cell method, and have no obvious discharge platform at all, which is corresponding to the conveniently reported results. [10] Comparatively, the PFcPy exhibits a 43.2 mAh g^{-1} capacity at the initial cycle on the same conditions, which is 60.1% of the theoretical capacity (71.8 mAh g^{-1}) (considering that PPy has no contribution to the total capacity, due to having no redox peaks occurring in the CV curve of Fig. 4(c)). Meanwhile, it is noteworthy that a flat voltage plateaus is obviously observed in the charge–discharge curves of the PFcPy, which is ascribed to the redox characteristics of organometallic ferrocene.

Further, the ferrocene-contained pyrrole (FcPy) and pyrrole are copolymerized to prepared P(FcPy-co-Py), and the electrochemical and charge/discharge properties of the obtained copolymer as an cathode for Li-ion battery are investigated. From the plot, we can observe that the initial discharge capacity of copolymer is further improved to about 68.1 mAh g^{-1}, which is obviously

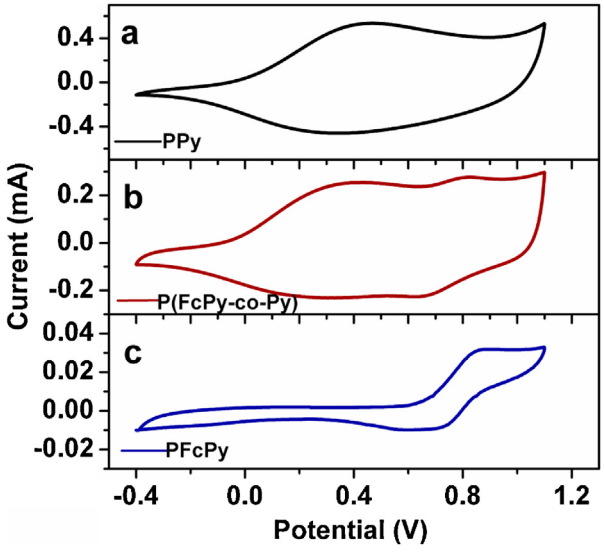

Fig. 4. Cyclic voltammograms (CV) of (a) PPy, (b) P(FcPy-co-Py) and (c) PFcPy in 0.1 M $LiClO_4/CH_3CN$ versus Ag/AgCl at the scan rate of 25 mV s^{-1}.

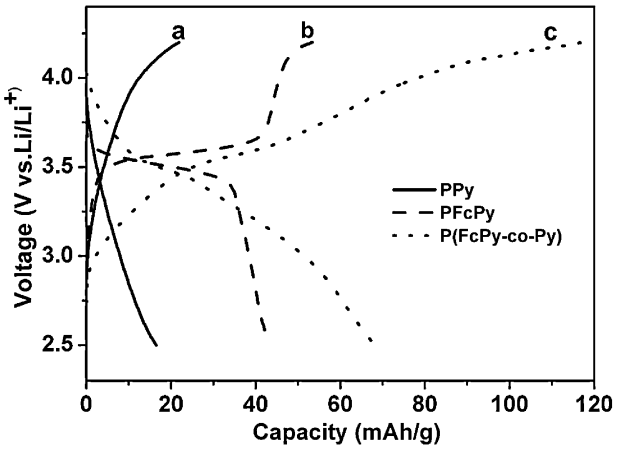

Fig. 5. Initial charge/discharge profiles of (a) PPy, (b) PFcPy and (c) P(FcPy-co-Py) electrodes material at a constant current of 20 mA g^{-1} between 2.5 and 4.2 V in $LiPF_6$ EC/DMC (v/v, 1:1) electrolyte versus Li/Li^+.

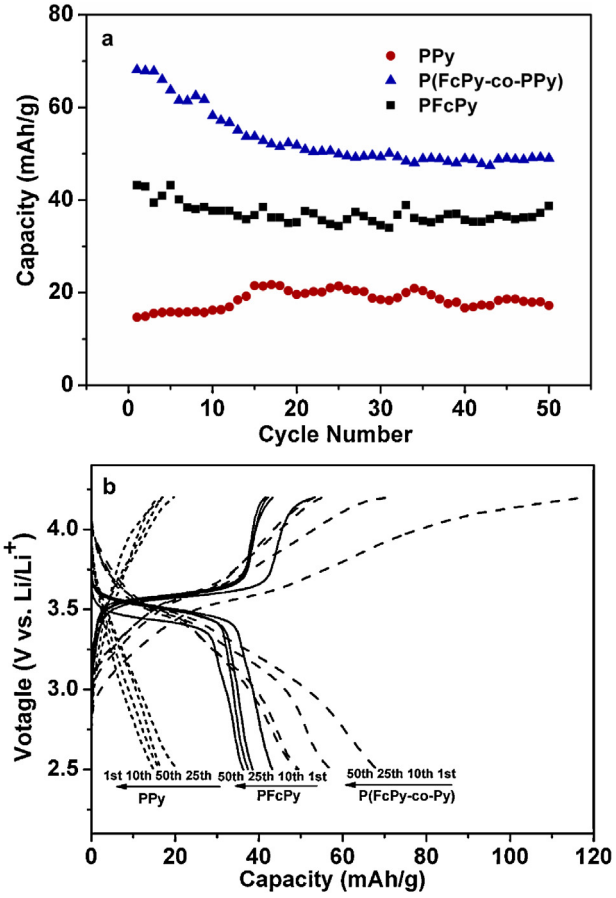

Fig. 6. (a) Cycling stability of the polymer electrodes material at a constant current of 20 mA g^{-1} between 2.5 and 4.2 V in $LiPF_6$ EC/DMC (v/v, 1:1) electrolyte versus Li/Li^+, (b) discharge profiles of PPy, P(FcPy-co-Py) and PFcPy.

enhanced as compared with those of PPy and PFcPy. We attribute this enhanced capacity to the contribution of redox-active ferrocene, as well as the improved doping level in the PPy main chain by the resonance electron-donating effect of the side chain group, which may improve the electron delocalization along the PPy main chain as proved by UV–vis spectra. Besides, loose structure of the P(FcPy-co-Py) particles is also in favor of the contact of electrode-active material and electrolyte, which improves the utilization of electrode-active material, resulting in the increase of specific capacity. Moreover, an improved discharge voltage plateau with a short voltage plateau near 3.5 V is exhibited comparing with that of PPy, which can be ascribed to the Fe^{III}/Fe^{II} redox couple of the ferrocene group, indicating that copolymer carries out two redox conversion during the charge/discharge process.[10] Specially, we catch sight of the difference between charge and discharge capacities of the initial process, in which the charge capacity (about 115 mAh g^{-1}) is much higher than the discharge capacity. This may be due to a volumetric change of the polymer during the initial charging process, which leads to degradation of the electrode contact and reduction of coulomb efficiency.

The cycling stability of the as-prepared polymers cathode is also examined, and the results are shown in Fig. 6(a). It is found that PPy, P(FcPy-co-Py) and PFcPy electrodes all show the unstable cycling performance after 50 cycles, which is decided by the nature of organic-based material electrode. Moreover, the cycling stability testing of P(FcPy-co-Py) exhibits a serious capacity degeneration in the initial 10 cycles, while the capacity of the following cycles maintains relatively stable. The initial capacity degeneration is possibly caused by the seriously re-aggregation of P(FcPy-co-Py)

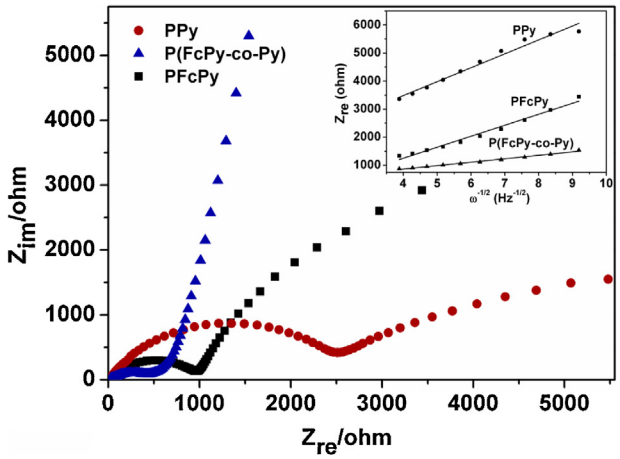

Fig. 7. EIS of PPy, P(FcPy-co-Py) and PFcPy sample in Li/Electrolyte/Sample configuration [Inset: Plot between Z_{re} and $\omega^{-1/2}$ for PPy, P(FcPy-co-Py) and PFcPy].

during the initial 10 charge–discharge cycles, due to the pristine looser stacking micro-structure of P(FcPy-co-Py) than those of PPy and PFcPy. Fig. 6(b) further presents the charge–discharge profile of the as-prepared polymers after 1st, 25th and 50th cycles. Even at 50th cycles, three electrodes still displays obviously stable voltage plateau, implying that PPy-based electrodes has a lower polarization during the charge–discharge process.

Fig. 7 shows electrochemical impedance spectra of pristine PPy, P(FcPy-co-Py) and PFcPy. The impedance spectra can be explained on the basis of an equivalent circuit with electrolyte resistance (R_e), charge transfer resistance (R_{ct}), double layer capacitance and passivation film capacitance (*CPE*) and Warburg Impedance (Z_w) [28,29]. In these impedance plots, the initial intercept of the spectrum at the Z_{re} axis in high frequency corresponds to the resistance of the electrolyte (R_e). The semicircles at low impedance frequencies represents the charge-transfer reaction resistance (R_{ct}), while the straight lines at low frequencies indicates the Warburg impedance(Z_w), which displays the diffusion-controlled process. As can be seen in the figure, the R_e is almost same for the cells with different cathode material, indicating that no significant change in ionic conductivity of the electrolyte or mobility of ions with the different cathode-based cell during the cycling process. However, R_{ct} varied with different cathode: 2510 Ω for PPy-based electrode and 963.8 Ω for PFcPy-based electrode. Specially, the R_{ct} of P(FcPy-co-Py) is only 433.0 Ω, which is the lowest of the three. This may ascribed to the porous and loosing structure of the copolymer which make electrolyte penetration easy and provide a higher surface area during redox. At the low frequency region, the straight line indicates the Warburg behavior, which is associated with diffusion process of Lithium-ions in the cathode material. The diffusion co-efficient of Lithium-ions could also be calculated by following relation (Eq. (1)) at low frequency [30,31]:

$$D = R^2T^2/(2A^2n^4F^4C^2\sigma^2) \quad (1)$$

$$Z_{im}\,\alpha\,\delta\omega^{1/2} \quad (2)$$

where R is the universal gas constant (8.314 J mol^{-1} k^{-1}), T is the temperature in Kelvin (K), A is the surface area of the cathode (cm^2), n is the number of electron per molecule during oxidation or reduction, F is the Faraday constant (96,485 C mol^{-1}), C is the concentration of lithium-ions in the cathode material (mol cm^{-3}) and σ is the Warburg factor (Ω $s^{1/2}$); which can be determined by plotting Z_{re} vs. $\omega^{-1/2}$ in the lower frequency region (Eq. (2)). The inset of Fig. 7 shows the relation between Z_{re} and frequency ($\omega^{-1/2}$) for PPy, PFcPy and P(FcPy-co-Py) samples respectively.

The slope of the curve determines σ and the intercept of the real component of impedance (Z_{re}) will produce R_{ct} value. The diffusion coefficient of lithium-ions in PPy, PFcPy and P(FcPy-co-Py) are found to be 1.34×10^{-15} cm^2 s^{-1}, 2.20×10^{-16} cm^2 s^{-1} and 4.53×10^{-15} cm^2 s^{-1} respectively. This suggests that the copolymer of P(FcPy-Co-Py) is more effective in improving chemical diffusion of Lithium-ion, which is according with the observation of both UV–vis spectra and SEM image.

4. Conclusion

A pyrrole derivative (FcPy) having a pendant ferrocene unite had been synthesized. The series of the conducting homopolymer and copolymer based on pyrrole and FcPy were obtained by chemical oxidation polymerization. For PFcPy, the polymer only exhibited the electrochemical characteristics of ferrocene pendant group with the 43.2 mAh g^{-1} of discharge capacity and a well-defined voltage plateau. And the PPy character had not been found due to seriously torsion polymer backbone by large steric effect of FcPy, which impaired the characteristics of PPy molecular. Comparatively, the charge/discharge properties of copolymer of FcPy and pyrrole (P(FcPy-co-Py)) obtained by the same process had been investigated, and it exhibited an obviously improved discharge capacity of 68.1 mAh g^{-1} as well as the improved discharge platform, which were ascribed to the resonance doping effect of pendant group, the advanced electrochemical nature of ferrocene moiety and the loose morphology of copolymer.

Acknowledgements

The authors gratefully thank the National Natural Science Foundation of China (NSFC, no. 51003095, no. 51103132) and Research on Public Welfare Technology Application Projects of Zhejiang Province, China (2010C31121) for financial support. This work also was supported by the analysis and testing foundation of Zhejiang University of Technology.

References

[1] J.M. Tarascon, M. Armand, Issues and challenges facing rechargeable lithium batteries, Nature 414 (2001) 359.
[2] Y. Nishi, Lithium ion secondary batteries: past 10 years and the future, Journal of Power Sources 100 (2001) 101.
[3] M. Armand, J.M. Tarascon, Building better batteries, Nature 451 (2008) 652.
[4] J.W. Park, J.Y. Eom, H.S. Kwon, Fabrication of Sn—C composite electrodes by electrodeposition and their cycle performance for Li-ion batteries, Electrochemistry Communications 11 (2009) 596.
[5] L. Taberna, S. Mitra, P. Poizot, P. Simon, J.M. Tarascon, High rate capabilities Fe_3O_4-based Cu nano-architectured electrodes for lithium-ion battery applications, Nature Materials 5 (2006) 567.
[6] H.Y. Chen, M. Armand, G. Demailly, F. Dolhem, P. Poizot, J.M. Tarascon, From biomass to a renewable $Li_xC_6O_6$ organic electrode for sustainable Li-ion batteries, ChemSusChem 1 (2008) 348.
[7] P. Novák, K. Müller, K.S.V. Santhanam, O. Haas, Electrochemically activepolymers for rechargeable batteries, Chemical Reviews 97 (1997) 207.
[8] M. Armand, S. Grugeon, H. Vezin, S. Laruelle, P. Ribière, P. Poizot, J.M. Tarascon, Conjugated dicarboxylate anodes for Li-ion batteries, Nature Materials 8 (2009) 120.
[9] T. Suga, S. Sugita, H. Ohshiro, K. Oyaizu, H. Nishide, P- and n-type bipolar redox-active radical polymer: Toward totally organic polymer-based rechargeable devices with variable configuration, Advanced Materials 23 (2011) 751.
[10] K.S. Park, S.B. Schougaard, J.B. Goodenough, Conducting-polymer/iron-redox-couple composite cathodes for lithium secondary batteries, Advanced Materials 19 (2007) 848.
[11] Y. Su, Y. Niu, Y. Xiao, M. Xiao, Z. Liang, K. Gong, Novel conducting polymer poly[bis(phenylamino)disulfide]: synthesis, characterization, and properties, Journal of Polymer Science Part A: Polymer Chemistry 42 (2004) 2329.
[12] T. Suga, H. Konishi, H. Nishide, Photocrosslinked nitroxide polymer cathode-active materials for application in an organic-based paper battery, Chemical Communications 17 (2007) 1730.
[13] J. Qu, T. Katsumata, M. Satoh, J. Wada, T. Masuda, Poly(7-oxanorbornenes) carrying 2 2,6,6-tetramethylpiperidine-1-oxy (TEMPO) radicals: synthesis and charge/discharge properties, Polymer 50 (2) (2009) 391.
[14] K. Tamura, N. Akutagawa, M. Satoh, J. Wada, T. Masuda, Charge/discharge properties of organometallic batteries fabricated with ferrocene-containing polymers, Macromolecular Rapid Communications 29 (2008) 1944.
[15] M. Yao, H. Senoh, T. Sakai, T. Kiyobayashi, Redox active poly(N-vinylcarbazole) for use in rechargeable lithium batteries, Journal of Power Sources 202 (2012) 364.
[16] M. Yao, H. Senoh, S. Yamazaki, Z. Siroma, T. Sakai, K. Yasuda, High-capacity organic positive-electrode material based on a benzoquinone derivative for use in rechargeable lithium batteries, Journal of Power Sources 195 (2010) 8336.
[17] J. Desilvestro, W. Scheifele, O. Hass, In situ determination of gravimetric and volumetric charge densities of battery electrodes polyaniline in aqueous and nonaqueous electrolytes, Journal of the Electrochemical Society 139 (1992) 2727.
[18] T. Osaka, T. Momma, K. Nishimura, S. Kakuda, T. Ishii, Application of solid polymer electrolyte to lithium/polypyrrole secondary battery system, Journal of the Electrochemical Society 141 (1994) 1994.
[19] P. Novák, W. Vielstich, Performance of the low-current-density-synthesized polypyrrole in lithium cells containing propylene carbonate, Journal of the Electrochemical Society 137 (1990) 1681.
[20] A. Laforgue, P. Simon, C. Sarrazin, J.F. Fauvarque, Polythiophene-based supercapacitors, Journal of Power Sources 80 (1999) 142.
[21] C.C. Changa, L.J. Her, J.L. Hong, Copolymer from electropolymerization of thiophene and 3,4-ethylenedioxythiophene and its use as cathode for lithium ion battery, Electrochimica Acta 50 (2005) 4461.
[22] T. Saji, Y. Maruyama, S. Aoyagui, Electrode kinetic parameters for the redox systems $Mo(CN)_8^{3-}/Mo(CN)_8^{4-}$-$IrCl_6^{2-}/IrCl_6^{3-}$, $Fe(phen)_3^{3+}/Fe(phen)_3^{2+}$ and $Fe(C_5H_5)^{2+}/Fe(C_5H_5)_2$, Journal of Electroanalytical Chemistry 86 (1978) 219.
[23] J. Irena, B. Stanley, J. Angela, H.A. Robert, Redox history effects accompanying the electrochemical cycling of poly(vinylferrocene), Journal of Solid State Electrochemistry 8 (2004) 403.
[24] T. Morikita, T. Yamamoto, Electrochemical determination of diffusion coefficient of (-conjugated polymers containing ferrocene unit, Journal of Organometallic Chemistry 637 (2001) 809.
[25] T. Yamamoto, T. Morikita, T. Maruyama, K. Kubota, M. Katada, Poly(aryleneethynylene) type polymers containing a ferrocene unit in the π-conjugated main chain. Preparation, optical properties, redox behavior, and mössbauer spectroscopic analysis, Macromolecules 30 (1997) 5390.
[26] H.X. Qiu, Z.Y. Wang, Z.J. Shi, Z.N. Gu, J.S. Qiu, Synthesis and infrared spectroscopy characterization of ferrocene-filled double-walled carbon nanotubes, Acta Physico-Chimica Sinica 23 (9) (2007) 145l.
[27] W.Z. Zhang, X.W. Kan, S.F. Jiao, J.G. Sun, D.S. Yang, B. Fang, Electrochemical characteristics and catalytic activity of polyaniline doped with ferrocene perchlorate, Journal of Applied Polymer Science 102 (6) (2006) 5633.
[28] S. Rodrigues, N. Munichandraiah, A.K. Shukla, AC impedance and state-of-charge analysis of a sealed lithium-ion rechargeable battery, Journal of Solid State Electrochemistry 3 (1999) 397.
[29] F. Nobili, F. Croce, B. Scrosati, R. Marassi, Electronic and electrochemical properties of $Li_xNi_{1-y}Co_yO_2$ cathodes studied by impedance spectroscopy, Chemistry of Materials 13 (2001) 1642.
[30] X. Qin, X. Wang, J. Xie, L. Wen, Hierarchically porous and conductive $LiFePO_4$ bulk electrode: binder-free and ultrahigh volumetric capacity Li-ion cathode, Journal of Materials Chemistry 21 (2011) 12444.
[31] Y. Zhou, J. Wang, Y. Hu, R. O'Hayre, Z. Shao, A porous $LiFePO_4$ and carbon nanotube composite, Chemical Communications 46 (2010) 7151.